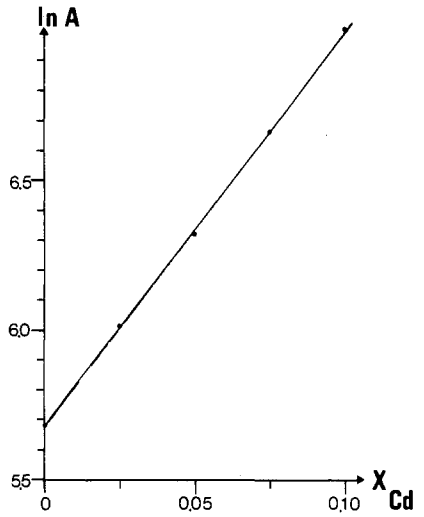

Figure 5. Viscosity Arrhenius parameter ln A of the molten salt mixtures as a function of the cadmium mole fraction (eq 8).

tion and V is again molar volume. The observed variation of V is, however, too small to account for the changes in A shown in Table V.

The variation of A and E with X_{Cd} may be expressed quantitatively by the equations (see Figures 4 and 5)

$$E = 59.680X_{Cd} + 27.142 \text{ kJ mol}^{-1} \quad (8)$$

$$\ln A(\text{cP}) = -13.30X_{Cd} - 5.674 \quad (9)$$

and the values of r are 0.9997 in both cases.

The simultaneous effects of T and X_{Cd} on ln η can be represented by the equation

$$\ln \eta = -5.674 - 13.30X_{Cd} + 3264T^{-1} + 7178X_{Cd}T^{-1} \quad (10)$$

Glossary

a, b	constants in eq 4, units cm^3 mol^{-1} K^{-1} and cm^3 mol^{-1}, respectively
A	viscosity preexponential factor (eq 6), cP
C	viscometer constant (eq 1), cSt s^{-1}
E	viscosity activation energy (eq 6), kJ mol^{-1}
p, q	constants in eq 5, cm^3 mol^{-1}
r	coefficient of correlation
R	gas constant, 8.314 J mol^{-1} K^{-1}
T	temperature, K
t	flow time (eq 1), s
V	molar volume (eq 3), cm^3 mol^{-1}
X_i	mole fraction of salt i in the mixture

Greek Letters

η	absolute viscosity, cP
ν	kinematic viscosity, cSt
ρ	density, g cm^{-3}
θ	temperature, °C

Literature Cited

(1) Blander, M. "Molten Salt Chemistry"; Interscience: New York, 1964.
(2) Gaira, J.; Stachowicz, L.; Suski, L. *J. Chem. Eng. Data* **1980**, *25*, 297.
(3) Sangster, J. M.; Abraham, M. C.; Abraham, M. *Can. J. Chem.* **1978**, *56*, 348.
(4) Timmermans, J. "Physico-Chemical Constants of Pure Organic Compounds"; Elsevier: New York, 1950.
(5) Kell, G. S. *J. Chem. Eng. Data* **1967**, *12*, 66.
(6) Timmermans, J. "The Physico-Chemical Constants of Binary Systems in Concentrated Solutions"; Interscience: New York, 1960; Vol. 4.
(7) Korson, L.; Drost-Hansen, W.; Millero, F. J. *J. Phys. Chem.* **1969**, *43*, 34.
(8) Sheely, M. L. *Ind. Eng. Chem.* **1932**, *24*, 1060.
(9) Janz, G. J.; Dampier, F. W.; Lakshminarayanan, G. R.; Lorenz, P. K.; Tomkins, R. P. T. "Molten Salts: Electrical Conductance, Density and Viscosity Data"; US National Bureau of Standards: Washington, DC, 1968; Vol. 1, NSRDS-NBS 15.
(10) Glasstone, S.; Laidler, K. J.; Eyring, H. E. "The Theory of Rate Processes"; McGraw-Hill: New York, 1941.
(11) Angell, C. A.; Moynihan, C. T. "Molten Salts: Characterization and Analysis"; Mamantov, G., Ed.; Marcel Dekker: New York, 1969; pp 315-75.

Received for review June 6, 1981. Accepted January 21, 1982. We thank the Natural Sciences and Engineering Research Council of Canada for financial aid.

Measurements of the Specific Heat, C_v, of Ethylene

Lloyd A. Weber

Thermophysical Properties Division, National Engineering Laboratory, National Bureau of Standards, Boulder, Colorado 80303

We have measured the specific heat, C_v, of gaseous and liquid ethylene in both the single- and two-phase regions, at pressures to 30 MPa. Temperatures varied from the triple point to 338 K, and densities varied from 0.6 to 2.8 times the critical value. The specific heats of the saturated liquid, C_σ, are derived. The results are compared with values calculated via the extended Benedict-Webb-Rubin (BWR) equation of state.

Introduction

The present work is part of a joint industry-government project to determine the thermodynamic properties of ethylene. This project consisted of two parts: acquisition of new experimental results (*1-8*), and the development of a model for the equation of state which would reproduce these results and which could be used to calculate reliable thermodynamic properties (*9*) over a wide range of temperature and pressure. The reader should refer to ref *9* for a complete set of references to work on ethylene.

The equation of state, in combination with the specific heat of the ideal gas, can be used to calculate the specific heat of the dense gas and the liquid through the use of well-known thermodynamic formulas. The accuracy of the results is generally rather poor, however, because the calculation depends upon the second derivative, $(\partial^2 P/\partial T^2)_\rho$, of the *PVT* surface. This quantity has a very small value, and it is often known with low accuracy even when high-quality *PVT* data are available. For calculations in the compressed liquid at low reduced temperatures, a further complication arises from the fact that the bulk of the integration (given in eq 1) required to calculate C_v must be performed inside the gas-liquid two-phase region where there are no data and where the behavior of the equation of state is thus unconstrained. As a result of these difficulties, calculated specific heats often diverge widely from the correct values in the liquid. If, however, measurements of specific heat are available, they may be combined with *PVT*

data by means of multiproperty fitting techniques (*10*) to yield an equation of state which is capable of reproducing specific heats and other thermodynamic properties within the experimental accuracy of the measurements.

We report here measurements of C_v of ethylene in the dense-gas and liquid phases and also for the gas–liquid two-phase system. The results are compared with calculations using the equation of state developed in this program. The specific heats of the saturated liquid are derived.

Experimental Section

Apparatus. The apparatus used here is the one originally described by Goodwin (*11*) with very few modifications. The calorimeter is a sphere of type 316 stainless steel 5 cm in diameter with a wall thickness of about 0.16 cm, having a nominal volume of about 72 cm^3. A stainless-steel filling capillary with an internal diameter of 0.015 cm is attached at the top of the sphere. A 100-Ω heater wire is wound directly on the outside of the sphere, and a lightweight, cylindrical copper case soldered to the sphere reduces radiation losses from the heater and also serves as an anchor point for two thermopiles controlling a guard ring and an adiabatic shield. Temperature was measured with a platinum resistance thermometer mounted in a tube welded to the bottom of the sphere, and voltage measurements were made with a six-dial potentiometer. Heater power input was measured electrically by using two potentiometers for the simultaneous measurement of voltage and current. An electronic counter was used to measure the heating time. A 10-min heating interval was used, and the power level was adjusted to give temperature increments varying from 2 to about 15 K. The calorimeter, surrounded by the guard ring and adiabatic shield, was mounted in an all-metal cryostat, a drawing of which appears in ref *11*.

The volume of the calorimeter was calibrated by gas expansion, and corrections were made for its variation with temperature and pressure. The amount of sample was determined from the density at the point on the *PVT* surface where the calorimeter was filled and sealed off by means of a stainless-steel valve. The density was calculated from the filling temperature and pressure, making use of the equation of state. Filling pressure measurements were made with an oil-operated dead-weight gauge. Pressures associated with each point could not be measured but were estimated by an iterative technique utilizing a preliminary equation of state.

The samples came from cylinders of ultrahigh-purity ethylene, obtained commercially, which were specially prepared for this project. (The stated purity of 99.999 mol % was verified in our laboratory.) The filling system and the calorimeter were evacuated and flushed several times with pure sample to remove other gases. Samples were passed through a molecular sieve trap to remove any water present.

Estimate of Uncertainties. The input power was measured several times during a heating interval and averaged; it was always constant to within about 0.1% and often to within 0.02%. Time intervals which were about 600 s are believed to be accurate to within several thousandths of a second. Overall accuracy is limited by the determination of ΔT (generally 1–5 mK) and the density (about 0.2%). The reliability of the basic calorimetric measurement, $Q/\Delta T$, was determined from measurements on the empty calorimeter. A dozen new measurements agreed with earlier data on the same apparatus to within about 0.07%, with an overall estimated uncertainty of 0.1%. The heat capacity of the empty calorimeter must be subtracted from the experimental heat capacity of the system. This has the effect of increasing the relative imprecision of the heat capacity of the sample, but it probably also tends to cancel out some of the small systematic errors inherent in any experimental measurement. The fraction of the total heat capacity due to the sample varied from 15% for the gas up to 67% for the dense-liquid data. Therefore, the overall maximum uncertainty in the basic data is estimated to vary from about 0.3% for the most dense samples to 0.75% for the least dense.

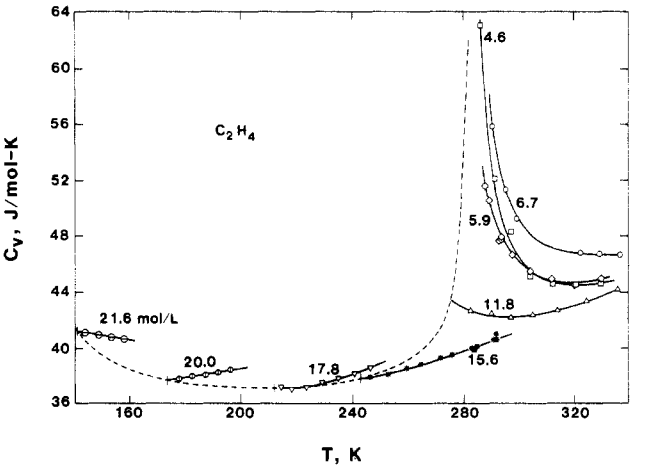

Figure 1. Single-phase specific heats of ethylene. Dashed line represents values for saturated-liquid conditions.

The results must also be adjusted for the *PV* work done by the sample when heated to a higher temperature and pressure. This correction is very small for the two-phase measurements, but it can be appreciable in the compressed liquid where the isochore slope, $(\partial P/\partial T)_\rho$, is quite large. It varied from 1% for the low-density measurements to 9% in the liquid. These corrections, which are given in detail in ref *12*, require the equation of state. The specific heat of the saturated liquid, C_σ, was calculated from the two-phase results, $C_v^{(2)}$, by means of eq 2. The corrections in eq 2 for the presence of the vapor are generally small below the normal boiling temperature, but they increase with the vapor pressure and amounted to as much as 20–30% for a few of the data near the critical temperature.

Results. The calorimeter was filled at a measured temperature and pressure, sealed off, cooled along the isochore to the vapor pressure curve, and cooled further along that curve to the starting temperature. Measurements often commenced in the two-phase region. The heat capacity rises to a maximum at the "breakthrough" temperature, at which point the meniscus vanishes from the calorimeter, and then drops discontinuously to a value corresponding to the single-phase fluid.

A total of 42 measurements were made on the two-phase system in the range 108–279 K, and 64 measurements were taken on the single-phase fluid. Eight densities varying from 4.6 to 21.4 mol dm^{-3} (ρ_c = 7.634) were used. Maximum temperatures and pressures were 340 K and about 30 MPa, respectively. Numerical results for the single-phase data are given in Table I. Pressures were not measured but were calculated by an iterative method using the equation of state. The two-phase data and derived saturated-liquid specific heats are shown in Table II. The vapor pressures are from the curve given by McCarty and Jacobsen (*9*). The equation of state used to process the specific heat data is a 32-term BWR equation, also from ref *9*. The results are shown graphically in Figures 1 and 2.

Discussion

Single-Phase Data. To our knowledge experimental C_v data have not been previously reported for ethylene. Therefore the only comparisons made here are with the values calculated via the equation of state, using the relationship

$$C_v(T,\rho) = C_v^\circ(T) - T\int_0^\rho (\partial^2 P/\partial T^2)_\rho \, d\rho/\rho^2 \qquad (1)$$

Table I. Single-Phase Specific Heats of Ethylene

T, K	ρ, mol dm⁻³	P, MPa	C_v, J mol⁻¹ K⁻¹	T, K	ρ, mol dm⁻³	P, MPa	C_v, J mol⁻¹ K⁻¹
285.886	4.63	5.126	59.07[a]	246.358	15.67	3.829	37.96
291.296	4.63	5.474	51.23[a]	252.733	15.65	7.204	38.16
297.325	4.63	5.856	47.94[a]	259.659	15.63	10.871	38.56
304.120	4.62	6.278	44.85	264.670	15.62	13.529	38.86
312.261	4.62	6.776	44.46	271.568	15.61	17.172	39.27
320.671	4.62	7.282	44.39	284.873	15.58	24.121	40.13
329.469	4.61	7.804	44.49	291.537	15.57	27.552	40.98
338.243	4.61	8.319	45.00	275.839	15.60	19.414	39.40
288.798	5.89	5.585	50.01[a]	283.777	15.58	23.551	39.85
293.405	5.89	5.980	47.73	291.502	15.57	27.532	40.60
287.721	5.89	5.492	50.74[a]	275.258	15.60	19.110	39.50
292.454	5.89	5.899	47.37	283.176	15.58	23.240	40.03
297.636	5.88	6.340	46.47	291.005	15.57	27.277	40.64
304.100	5.88	6.885	45.35	214.364	17.85	2.647	37.16
311.716	5.88	7.520	44.83	218.264	17.83	5.759	37.13
320.019	5.87	8.206	44.45	223.479	17.81	9.902	37.28
329.795	5.87	9.006	44.90	229.213	17.79	14.453	37.62
289.793	6.73	5.790	54.88	235.231	17.78	19.178	37.86
294.813	6.73	6.293	50.85	240.828	17.76	23.518	38.23
298.731	6.73	6.684	48.93	246.383	17.74	27.767	38.66
322.290	6.72	9.016	46.74	178.068	20.01	5.569	37.85
329.075	6.71	9.682	46.68	182.726	19.99	11.053	38.06
336.481	6.71	10.406	46.60	187.339	19.97	16.479	38.12
282.622	11.82	6.145	42.65	191.736	19.95	21.590	38.30
289.904	11.81	7.948	42.38	196.289	19.93	26.807	38.44
297.145	11.80	9.775	42.15	144.122	21.60	4.593	41.10
304.989	11.79	11.783	42.29	148.698	21.57	11.633	40.91
314.121	11.78	14.144	42.67	153.288	21.54	18.695	40.75
324.645	11.77	16.884	43.32	157.837	21.52	25.593	40.57
335.896	11.76	19.819	44.13				

[a] Inconsistent data (see text).

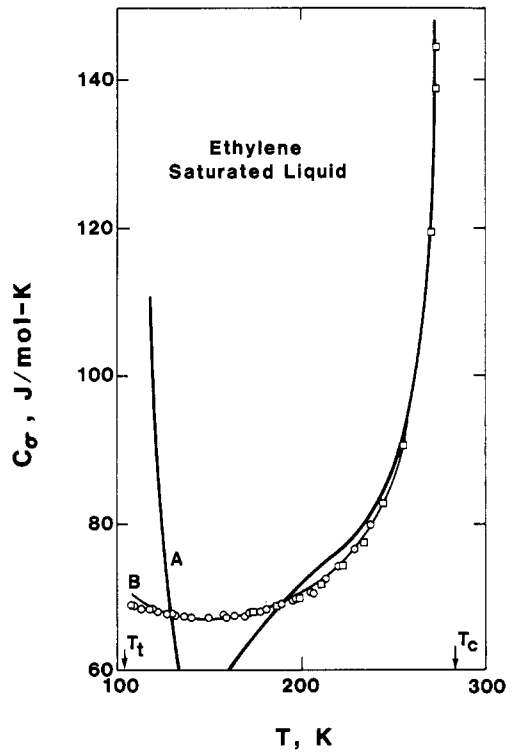

Figure 2. Specific heats of saturated liquid ethylene. Curves show values calculated by equation of state: (A) without specific heat data included; (B) with specific heat data.

where $C_v^\circ(T)$ is the ideal-gas specific heat. The values for $C_v^\circ(T)$ were calculated from an equation given in ref 9. Comparisons were made with values calculated with an early form of the equation of state constructed without benefit of the C_v data, and also with the final equation utilizing all of the data. For the purpose of the discussion, it is convenient to divide the data into three groups according to density.

Table II. Two-Phase Specific Heats of Ethylene

T, K	P, MPa	$C_v^{(2)}$, J mol⁻¹ K⁻¹	C_σ, J mol⁻¹ K⁻¹
	ρ = 15.65 mol dm⁻³		
109.301	0.0003	68.94	68.92
119.592	0.0013	68.40	68.36
129.841	0.0043	67.93	67.83
139.876	0.0117	67.45	67.27
149.676	0.0267	67.49	67.20
159.356	0.0538	67.66	67.24
168.862	0.0983	68.00	67.47
178.215	0.1658	68.65	68.02
186.558	0.2518	69.42	68.76
195.662	0.3801	70.21	69.62
204.595	0.5480	71.03	70.65
213.008	0.7510	72.49	72.48
220.080	0.9601	73.67	74.18
228.558	1.2630	75.15	76.63
236.905	1.6233	76.66	79.66
	ρ = 5.88 mol dm⁻³		
173.499	0.1284	74.41	68.04
186.377	0.2496	78.03	68.67
198.758	0.4332	82.54	69.90
210.756	0.6921	87.71	71.66
222.301	1.0337	93.58	74.20
233.442	1.4659	99.70	77.27
244.181	1.9932	107.43	82.60
255.457	2.6822	116.31	90.54
274.553	4.2320	141.00	136.03
271.352	3.9334	133.93	118.98
275.437	4.3177	143.65	143.12
279.424	4.7225	151.46	202.46
	ρ = 17.84 mol dm⁻³		
157.366	0.0470	67.51	67.34
163.629	0.0713	67.42	67.24
172.385	0.1206	67.87	67.70
181.041	0.1919	68.27	68.16
189.574	0.2900	68.96	69.01
197.984	0.4194	69.66	69.98
197.902	0.4180	69.64	69.95
206.188	0.5829	70.52	71.24
	ρ = 21.61 mol dm⁻³		
108.412	0.0003	68.78	68.82
113.010	0.0005	68.44	68.49
117.562	0.0010	68.31	68.37
122.074	0.0018	68.06	68.12
127.090	0.0032	67.66	67.73
131.544	0.0052	67.53	67.60
135.966	0.0081	67.39	67.46

Low-Density Data. Three runs were made at subcritical densities 4.6, 5.9, and 6.7 mol dm⁻³ in the temperature range 285–339 K (T_c = 282.343 K). Comparison with results of the early form of the equation revealed systematic disagreements of about 5% between calculated and experimental values. Some of the data fell within the critical region (defined here as $T_c \pm 5\%$, $\rho_c \pm 40\%$), where the disagreement ran as high as 20%. This behavior is expected with an analytic equation such as the BWR. In addition, some of the data in this region seemed to be mutually inconsistent. Therefore, although these data are reported in Table II, they should be viewed with some reservation. The final version of the equation yielded calculated C_v's which agreed with the measured values within 1–3% for temperatures above 300 K. This is considered to be a reasonably satisfactory agreement in this range.

Intermediate Densities. Three runs were made at densities 11.8, 15.6, and 17.8 mol dm⁻³, covering the temperature range 214–335 K. Calculated values from the early version of the equation of state showed deviations ranging from −4% to +4%. In general, however, the agreement was considerably

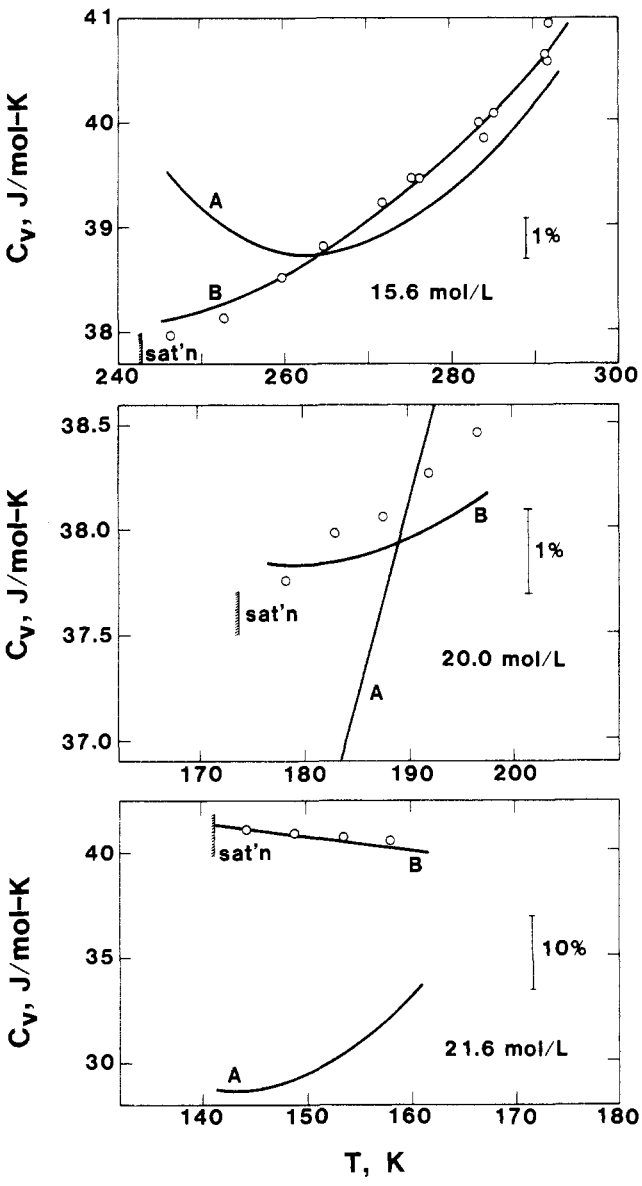

Figure 3. Three examples of single-phase specific heat data compared with calculated values. Curves defined as in Figure 2.

better than for the low-density data. Inclusion of these data in the fit of the later equation reduced these deviations to −0.4% to +0.75%, nearly a tenfold improvement, to deviations which approximated the uncertainties in the data themselves.

High Densities. Two densities, 20.0 mol dm^{-3} (178–196 K) and 21.6 mol dm^{-3} (144–158 K) were measured. Although the densities were similar, the temperature range was different. These liquid densities illustrate well the problems discussed in the Introduction. At 20 mol dm^{-3} the early version of the equation calculated values which disagreed by only 5.6% to −2.3%; however, they were highly skewed with respect to the data. At the higher density the calculated values were incorrect by 20–30%. This problem became even worse at lower temperatures, as shown below. When these runs were included as input data, however, the later equation showed an average disagreement of only 0.4%, a remarkable improvement. The fit of the *PVT* data was not noticeably changed. The agreement between calculated and experimental values for three isochores is shown in Figure 3.

Two-Phase Data. Four of the eight experimental densities included data for the gas–liquid two-phase system. These data, designated $C_v^{(2)}(\bar{\rho},T)$, are functions of the average, or filling, density $\bar{\rho}$. Therefore, each density was checked separately by fitting the data with a low-order function. These fits showed that the data have a precision of about 0.1%. They also allowed curvature corrections to be made in order to adjust for the fact that the experimental measurements are finite differences rather than derivatives. These corrections were generally quite small, but they became larger near the critical point, amounting to as much as 2% for several points.

The specific heat of the saturated liquid, C_σ, was then calculated by means of the relationship

$$C_\sigma(T) = C_v^{(2)}(\bar{\rho},T) - \left(\frac{T}{\rho_\sigma}\right)\left[\left(\frac{d\rho}{dT}\right)_\sigma\left(\frac{dP}{dT}\right)\frac{1}{\sigma\rho_\sigma} + \left(\frac{\rho_\sigma}{\bar{\rho}} - 1\right)\left(\frac{d^2P}{dT^2}\right)_\sigma\right] \quad (2)$$

where the subscript σ refers to property values for the saturated liquid. The results are shown in Table II and Figure 2. The value of C_σ depends only on the temperature, and therefore all of the data could be represented from the triple point to the critical point by a single curve of the form

$$C_\sigma = A + BT + CT^2 + DT^3 + ET/(T_c - T)^{0.6} \quad (3)$$

where $A = 0.86173 \times 10^2$, $B = -0.27230$, $C = 0.65374 \times 10^{-3}$, $D = -0.23129 \times 10^{-6}$, $E = 0.99834$, and $T_c = 282.343$ K (T in K and C_σ in J mol^{-1} K^{-1}). The average relative deviation is 0.20%, which is equal to the quality of the fit of the equation of state used to determine the amount of sample for each run.

No other data on the C_σ of ethylene have been reported. Values calculated from the early version of the equation of state agreed fairly well (−2% to −4%) with the data above the normal boiling temperature (169.409 K). Below this temperature, however, the calculated values showed wide excursions, from +17% near 140 K to −270% near the triple point. When these data were included in the fitting process, the later equation produced calculated values which agreed with the data to within about 1% from the triple point to very near the critical point. We regard this improvement as being very significant because it indicates that the final equation of state in ref *9* can be counted upon to give reliable values for the thermodynamic properties in the low-temperature liquid state.

Conclusions

We have presented the results of new measurements of C_v of ethylene in both the single- and two-phase regions. The precision of the data agrees with estimations based upon the capability of our calorimeter and the quality of the equation of state used to determine the density. We have shown how these data have been utilized to provide an improved equation of state. The improved equation reproduces the measurements almost within the experimental error in most regions.

Acknowledgment

This work was a joint industry–government project under the sponsorship of Celanese Chemical Co., Cities Service Oil Co., Continental Oil Co., Gulf Research and Development, Mobil Chemical Co., Monsanto Polymers and Petrochemicals Co., Phillips Chemical Co., Union Carbide, and the National Bureau of Standards.

Literature Cited

(1) Douslin, D. R.; Harrison, R. H. *J. Chem. Thermodyn.* **1976**, *8*, 301.
(2) Hastings, J. R.; Levelt Sengers, J. M. H.; Balfour, F. W. *J. Chem. Thermodyn.* **1980**, *12*, 1009–45.
(3) Levelt Sengers, J. M. H., US National Bureau of Standards, private communication May 1979.
(4) Straty, G. C. *J. Chem. Thermodyn.* **1980**, *12*, 709.
(5) Dregulas, E. K.; Stavtzev, A. F., private communication, Sept 1979.

(6) Gammon, B. E., presented at the Advisory Committee Meeting of the Joint Industry–Government Ethylene Project, Boulder, CO, Dec 1978.
(7) Hejmadi, A. V.; Powers, J. E., private communication, July 1979.
(8) Koziov, A., USSR Academy of Sciences, private communication.
(9) McCarty, R. D.; Jacobsen, R. T. *NBS Tech. Note (U.S.)* **1981**, No. 1045.
(10) Hust, J. G.; McCarty, R. D. *Cryogenics* **1967**, *7*, 200.
(11) Goodwin, R. D. *J. Res. Natl. Bur. Stand. Sect. C* **1961**, *65*, 231.
(12) Goodwin, R. D.; Weber, L. A. *J. Res. Natl. Bur. Stand. Sect. A* **1969**, *73*, 15.

Received for review July 27, 1981. Accepted January 19, 1982.

NEW COMPOUNDS

Synthesis and Reactions of 2-Mercaptobenzothiazole Derivatives of Expected Biological Activity. 2†

Abou El-Fotooh G. Hammam* and Nabil M. Youssif

National Research Centre, Dokki, Giza, Arab Republic of Egypt

The amides and anilides of benzothiazol-2-ylthioacetic acid and 3-(benzothiazol-2-ylthio)propanoic acid were prepared by the reaction of the corresponding acid chlorides with amines and anilines. Also the arylhydrazones, the cycloalkanone hydrazones, and pyrazoline derivatives were prepared.

The literature (*1–3*) reveals that substituted benzothiazoles possess anticonvulsant activity and these inhibit monoamine oxidase activity of rat brain homogenate. The following compounds are prepared to test them for biological activity.

Experimental Section

Satisfactory elemental analyses were found.

Benzothiazol-2-ylthioacetic Acid (IIa). A mixture of 1.7 g (0.01 mol) of 2-mercaptobenzothiazole and 0.8 g (0.01 mol) of chloroacetic acid in 50 mL of ethanolic potassium hydroxide (1 g of KOH in 50 mL of ethanol 70%) was refluxed for 3 h. The ethanol was evaporated, and the precipitate formed was dissolved in water and acidified with hydrochloric acid. The precipitate formed was collected and crystallized from ethanol: mp 135 °C; yield 70%.

3-(Benzothiazol-2-ylthio)propanoic Acid (IIb). This compound was prepared as above by replacing the chloroacetic acid with 3-bromopropanoic acid and crystallizing from ethanol: mp 150 °C; yield 83%.

4-(Benzothiazol-2-ylthio)butanoic Acid (IIc). 2-Mercaptobenzothiazole (1.7 g) was dissolved in a solution of 0.3 g of sodium metal in about 15 mL of absolute ethanol. The mixture was refluxed for 3 h. The ethanol was distilled off, and the white mass formed was dissolved in hot water and filtered. The filtrate was acidified with hydrochloric acid. The solid formed was collected and crystallized from ethanol: mp 120 °C; yield 67%. The IR spectra of compounds II showed absorption at 1705 cm^{-1} (COOH).

Amides (III). General Procedure. A mixture of 2 g of the acid (IIa,b), 5 mL of thionyl chloride, and 20 mL of dry benzene was refluxed for 2 h. The excess of thionyl chloride and benzene was distilled off, and the remaining oil was dissolved in dry benzene, cooled and quickly treated with 2 g of the amine, refluxed for 2 h, and left overnight. The reaction mixture was filtered, the precipitate was washed with ether, and the combined filtrate and washing were extracted with dilute hydrochloric acid and then with sodium carbonate solution. The ethereal solution was dried and evaporated. The residue was triturated with light petroleum ether, and the solid formed was collected and crystallized from the proper solvent (see Table I).

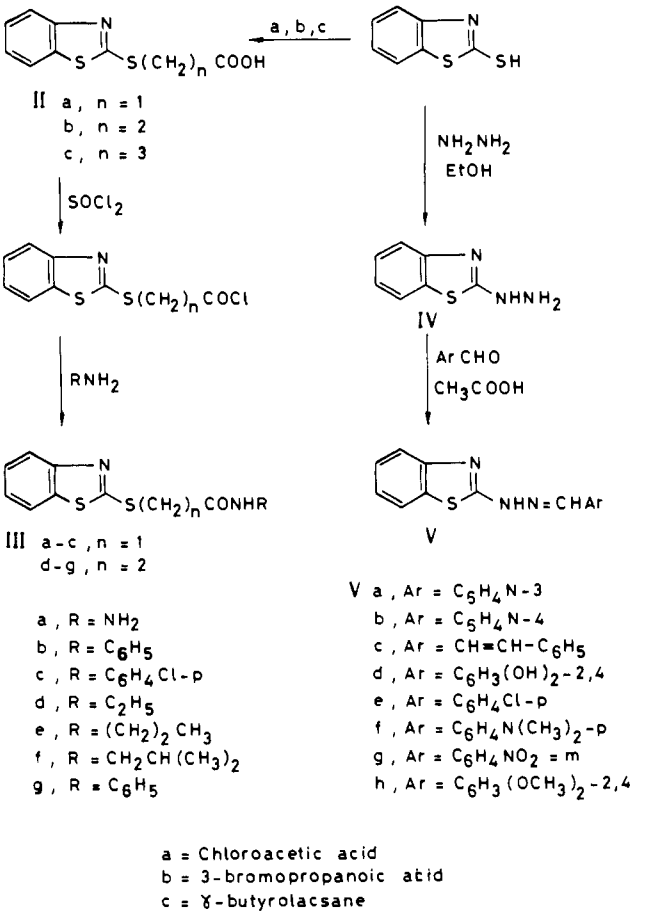

Anilides. The acid chlorides were prepared as in the General Procedure and then treated with aniline and worked up as above (see Table I).

† For part 1, see ref *4*.

0021-9568/82/1727-0207$01.25/0